IEEE Access
Multidisciplinary | Rapid Review | Open Access Journal

Received April 28, 2020, accepted May 6, 2020, date of publication May 12, 2020, date of current version May 27, 2020.

Digital Object Identifier 10.1109/ACCESS.2020.2994050

An Improved Spatio-Temporal Kriging Interpolation Algorithm and Its Application in Slope

HAIPING XIAO[1], ZHENCHAO ZHANG[1], LANLAN CHEN[2], AND QIMIN HE[3]
[1]School of Architectural and Surveying & Mapping Engineering, Jiangxi University of Science and Technology, Ganzhou 341000, China
[2]College of Applied Science, Jiangxi University of Science and Technology, Ganzhou 341000, China
[3]School of Environment Science and Spatial Informatics, China University of Mining and Technology, Xuzhou 221116, China

Corresponding author: Haiping Xiao (415562281@qq.com)

This work was supported in part by the Science and Technology Research Project of the Education Department of Jiangxi Province under Grant GJJ190446 and Grant GJJ191591, and in part by the High Level Talents Research Start-Up Project of the Jiangxi University of Science and Technology under Grant jxxjbs19032.

ABSTRACT Slope stability analysis based on the deformation monitoring data has been commonly used to predict and warn slope disasters. However, due to breakdown of the monitoring equipment or restrictions and interferences of internal and external factors in the area, the loss of data is unavoidable during the process of the slope monitoring. This problem can be solved by the spatio-temporal Kriging interpolation algorithm. However, the subjective factors and theoretical semi-variogram of variogram models, and many parameters estimation may lead to low interpolation precision and poor calculation efficiency. In this paper, a hybrid spatio-temporal interpolation algorithm was presented by combining the improved adaptive genetic algorithm (IAGA) with the spatio-temporal Kriging interpolation method, and it was applied to monitor the deformation of HP1 slope in Yuebao open-pit mine. The results showed that the interpolation precision of the proposed method was about 1 times higher than that of the traditional spatio-temporal Kriging method and the spatio-temporal method of Gaussian process regression method. In addition, after the interpolation analysis of the missing part of the monitoring data, the maximum cumulative displacement of all monitoring points was around 35.8 mm, and the rate of the displacement deformation didn't exceed 2 mm/d for three consecutive days. The deformation trend was basically consistent with the actual slope. It shows that the improved spatio-temporal Kriging interpolation algorithm (ISTKIA) has certain feasibility and reliability, and could provide a new idea for the research of related problems in related fields.

INDEX TERMS Slope deformation monitoring, spatio-temporal Kriging interpolation, ISTKIA, stability analysis.

I. INTRODUCTION

With increasing demand for mineral resources during social and economic development in China, mineral enterprises continue to carry out mining activities, which results in a large number of open-pit slopes. According to incomplete statistics, there are 62,854 metal and non-metal mines in China, in which 54,746 are open-pit mines, accounting for 87.1% of all mines. Among them, 51,953 are small and medium open-pit mines, taking up about 94.9% [1]. However, the open-pit slopes, especially the small and medium open-pit slopes, occur various accidents and disasters under the influence of natural environment, external disturbance, as well as poor enterprise management and serious shortage of safety investment and etc., which have brought huge hidden danger to life and property security [2]–[4]. In order to ensure safety production and management in mines, scholars both at home and abroad have done a lot of research, especially researches on the slope deformation monitoring [5], [6]. The deformation monitoring data are commonly used to analyze the slope stability and forecast slope disasters.

Restricted by funding, equipment, technology and observational conditions, most of the small mining enterprises adopt traditional monitoring methods to monitor slope deformation

The associate editor coordinating the review of this manuscript and approving it for publication was Guangdeng Zong.

in practical application. Some mining enterprises also use advanced devices such as measuring robots or GNSS for slope monitoring [7], [8], but the number of monitoring points and obtained monitoring data are generally hard to meet the needs of scientific research and engineering application. Some monitoring points are often damaged or missed, resulting in the loss of data, and affect the effective analysis of the slope stability. At present, it has become an active research field to solve the problems of data loss and scarcity. Domestic and foreign scholars have carried out a lot of research on remote sensing data [9], temperature [10], rainfall [11], soil moisture and temperature [12], PM2.5 [13], pollutant diffusion [14], ionosphere [15], dam deformation [16] and etc. Shen *et al.* [17] have comprehensively analyze the interpolation processing of the missing information of remote sensing data, and summarized four main classes: 1) spatial-based methods; 2) spectral-based methods; 3) temporal-based methods; and 4) hybrid methods. Results have been achieved in the research of the missing data interpolation, and could provide an important theoretical reference and technical support for the research of this paper.

To make up for and overcome the shortage or loss of the slope monitoring data, and accurately analyze the overall deformation trend and stability of the open-pit slope, it is necessary to interpolate the existing irregular, discontinuous, and limited monitoring data, which is useful to improve the integrity and continuity of the slope monitoring data, and support later data processing, slope stability analysis, and related scientific research. At present, there are three main classes of the research on the interpolation of the deformation monitoring data. The first classes only consider the relevance in the time domain, such as Lagrange interpolation method [18], Hermite interpolation method [19], and the spline interpolation method [20] and etc. These methods make use of the correlation of the data of the damaged points or missing points collected in different time. They can realize efficient interpolation, but it is easy to produce artifacts [21]. The slope is integral and composed of numerous points. There are a certain connections between points, and they are interdependent, rather than isolated individuals. However, these methods only consider the correlation of points in different time, and do not consider the influence of other monitoring points in the adjacent area. The second classes only consider the relevance in the spatial domain, such as the inverse distance weighting method and the spatial Kriging interpolation method [22]. Such methods utilize the correlations of the local or nonlocal information in the corrupted data itself. Although these methods consider the relationship between the points in the neighborhood, they do not study particularity of individual changes and the correlation of adjacent time data. Above all, these two classes of methods are one-sided and could affect the precision of interpolation data. According to a large number of practice and research results, the changes of the slope deformation monitoring data are related to both time attributes and spatial attributes. They have strong spatio-temporal correlations [23]. In view of this, some scholars have proposed a third kind of the spatio-temporal interpolation method which considers both the temporal correlations and the spatial correlations. Liu *et al.* [24] adopted an uneven spatio-temporal Kriging interpolation algorithm to analyze the landslide displacement. Lenda *et al.* [25] applied four different interpolation algorithms to build a surface model of the slope to analyze the progressive movement of the landslide. Wang and Zhang [26] and Wang *et al.* [27] used the spatio-temporal Kriging interpolation of Gaussian process regression and the spatio-temporal Kriging to interpolate the monitoring data for slope deformation analysis. The results showed that the root mean square error of the spatio-temporal Kriging interpolation was 40% higher than that of the spatial Kriging interpolation, while the average error was 55% higher, fully reflecting the spatio-temporal correlation of deformation monitoring points.

The analysis of the aforementioned spatio-temporal interpolation literatures indicates that the key to the precision of the spatio-temporal Kriging interpolation is the spatio-temporal variogram model. In practical application, the variogram model which is closest to the structural characteristics is selected artificially based on the semi-variogram of the experimental samples data. There are some limitations and shortages, such as subjective factors, theoretical semi-variogram function, and many estimated parameters, which may lead to low interpolation precision and poor calculation efficiency [28]. To optimize the model and improve calculation efficiency and time convergence, scholars both at home and abroad have carried out a lot of researches in the fields of spacecraft control [29], the treatment of viral mutations [30], vertical take-off and landing of helicopters [31], time stability [32] and etc., using nonlinear algorithms and models such as the genetic algorithm, Markov chain and etc. They have made abundant results, which could provide theoretical references and thoughts for our research. On the basis of fully considering spatio-temporal correlations of monitoring points, and in order to overcome such limitations, this paper aims to propose an improved spatio-temporal Kriging interpolation algorithm (ISTKIA) to realize the interpolation of the missing data and ensure the continuity and integrity of the slope monitoring data. The method will be applied in HP1 (the number of slope subjected to landslide in the study area) slope in Yuebao open-pit mine, in hope of decreasing production costs of enterprises, improving work efficiency, providing technical support and decision basis for slope disaster prevention, mitigation and relief, as well as offering new ideas for related researches.

The rest of this paper is arranged as follows. Section 2 introduces the proposed hybrid spatio-temporal interpolation algorithm based on the improved adaptive genetic algorithm (IAGA) and the spatio-temporal Kriging interpolation method. Section 3 describes the experiments undertaken to verify the reliability and feasibility of the proposed ISTKIA by comparing the precision with the traditional spatio-temporal Kriging interpolation method and the spatio-temporal interpolation algorithm of Gaussian process

regression. In Section 4, the missing data in monitoring are interpolated to analyze the change trend of the deformation monitoring points and the stability of the slope by taking the HP1 slope of Yuebao open-pit mine as an example. Finally, the paper summarizes the achievements and contributions of the research in Conclusions.

II. METHODLOGY

Ordinary Kriging is a reliable estimation method based on the continuous model of the random spatial variation for data interpolation [33], with the characteristics of unbiased estimation [34] and minimum variance of estimation error [35]. Given that Kriging model uses the preset global trend model and its approximate precision may not be optimal [36], the genetic algorithm and cross-validation were used to find out the optimal model of Kriging model and avoid the identification process falling into local optimum [37], [38]. Although interpolating missing data by spatio-temporal Kriging method fully considers the spatiotemporal correlations of monitoring points, there are still issues with variogram models, parameter estimation and a large amount of time for spatiotemporal modeling [39]. To overcome such shortcomings and limitations, this paper introduced the genetic algorithm with the advantage of finding global optimum solutions and proposed a hybrid spatio-temporal interpolation algorithm combining an improved adaptive genetic algorithm (IAGA) with the spatio-temporal Kriging interpolation method. It has great theoretical values and practical significance to make up for and overcome problems of the loss of slope monitoring data, and accurately analyze the stability and deformation trends of slopes in open-pit mines. The specific construction ideas are as follows.

A. THE PRINCIPLE OF THE SPATIAL KRIGING INTERPOLATION

The common spatial Kriging method is mainly based on correlation theories of variation functions and structural analysis. It takes limited known data of monitoring points as variables, and conducts linear unbiased optimal estimation for values of unsampled points. Its basic mathematical model is expressed by Eq.1:

$$Z(x_0) = \sum_{i=1}^{n} \lambda_i Z(x_i), \quad \sum_{i=1}^{n} \lambda_i = 1 \tag{1}$$

where $Z(x_0)$ is the discreet value at the unknown point x_0; $Z(x_i)$ is the monitored value of the unknown point at the known point x_i in the neighborhood; λ_i is the kriging weight and its value could be obtained by variation function; and n is the number of the known sample points. Therefore, in order to get discreet values of unknown points, the most key issue of Kriging interpolation is to get the weight coefficient λ_i by constructing the variation function. Then, the estimation value $\gamma^*(h)$ of the variation function $\gamma(h)$ could be obtained by the following Eq.2:

$$\gamma^*(h) = \frac{1}{2n(h)} \sum_{i=1}^{n(h)} [Z(x_i) - Z(x_i + h)]^2 \tag{2}$$

where $\gamma^*(h)$ is the estimation value of the unknown point; $Z(x_i)$ is the monitored value at the known point x_i in the neighborhood of the unknown point; $Z(x_i + h)$ is the monitored value, h apart with $Z(x_i)$; $n(h)$ refers to the number of data pair of the sample points of h.

B. THE PRINCIPLE OF THE SPATIO-TEMPORAL KRIGING INTERPOLATION

The spatio-temporal Kriging interpolation [40], [41] extends data from spatial to spatio-temporal domain, fully taking into account spatial and temporal relevance among monitoring points [42]. The spatio-temporal position function is: $Z(h_a, h_a) = Z(x, y, z, t)$ $(h_a = f(x, y, z))$, then the spatio-temporal Kriging interpolation model can be expressed as Eq.3:

$$Z^*\left(h_p, t_p\right) = \sum_{i=1}^{n(u,t)} \lambda_i Z\left(h_i, t_i\right), \quad \sum_{i=1}^{n(u,t)} \lambda_i = 1 \tag{3}$$

where $Z^*(h_p, t_p)$ is the estimated value of the unknown point p, $Z(h_i, t_i)$ is the monitored value of the known sample point i in the neighborhood of the unknown point p, $n(u, t)$ is the number of the known sample point pairs, λ_i is the Kriging weight coefficient that minimizes the interpolation error, which needs to meet minimum variance unbiased estimation, as shown in Eq.4.

$$\begin{cases} \min Var(Z^*(h_p, t_p) - Z(h_p, t_p)) \\ E((h_p, t_p) - Z(h_p, t_p)) = 0 \end{cases} \tag{4}$$

In the process of the spatio-temporal Kriging interpolation, the estimated values of the unknown points should be obtained. Therefore, the estimated value $\gamma^*(h_s, h_t)$ of the vriation function $\gamma(h_s, h_t)$ should be calculated according to Eq.5:

$$\gamma^*\left(h_s, h_t\right) = \frac{1}{2n\left(h_s, h_t\right)} \sum_{i=1}^{n(h_s,h_t)} \left[Z\left(h_i, h_i\right) - Z\left(h_i + h_s, h_i + h_t\right)\right]^2 \tag{5}$$

In Eq.5, $\gamma^*(h_s, h_t)$ is an estimated value of an unknown point; $Z(h_i, t_i)$ is the monitored value of the sample point i; $Z(h_i + h_s, t_i + h_t)$, h_s apart in space and h_t apart in time from $Z(h_i, t_i)$, is a monitoring value; h_s, h_t represent the spatial separation distance, respectively; $n(h_s, h_t)$ represents the number of the sample data point pairs,with the spatio-temporal separation distances of h_s, h_t.

Then, a commonly-used inseparable method was used to construct the variogram model of the spatio-temporal

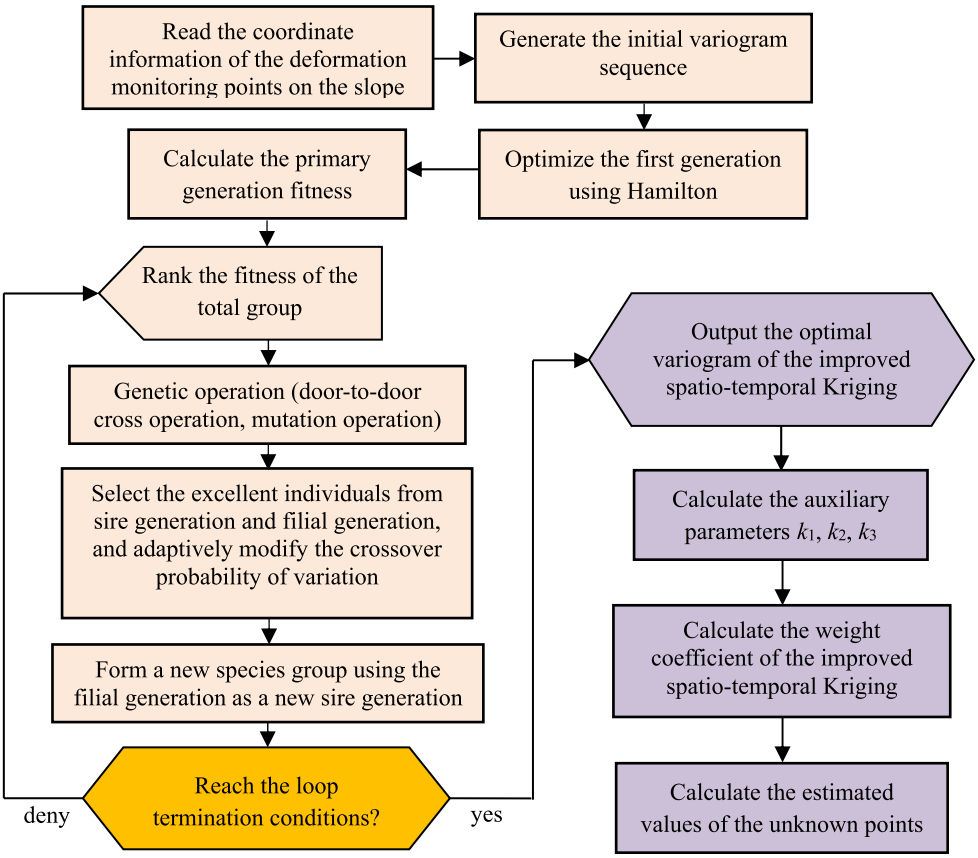

FIGURE 1. Calculation flow of the improved spatio-temporal Kriging interpolation algorithm (ISTKIA) based on IAGA.

Kriging. The model is shown in Eq.6.

$$\begin{cases} \gamma_{st}(h_s, h_t) = [(k_1 C_t(0) + k_2)]\gamma_s(h_s) \\ \quad + [(k_1 C_s(0) + k_3)]\gamma_t(h_t) - k_1\gamma_s(h_s)\gamma_t(h_t) \\ k_1 = [C_s(0) + C_t(0) - C_{st}(0,0)]/[C_s(0)C_t(0)] \\ k_2 = [C_{st}(0,0) - C_t(0)]/C_s(0) \\ k_3 = [C_{st}(0,0) - C_s(0)]/C_t(0) \end{cases} \tag{6}$$

In Eq.6, $\gamma_{st}(h_s, h_t)$ represents the spatio-temporal variation function; $\gamma_s(h_s)$ represents the spatial variogram; $\gamma_t(h_t)$ represents the time variation function; $C_{st}(0, 0)$, $C_s(0)$, $C_t(0)$ are the abutment values of the corresponding variograms, respectively; k_1, k_2 and k_3 are auxiliary parameters.

C. THE IMPROVED SPATIO-TEMPORAL KRIGING INTERPOLATION ALGORITHM BASED ON IAGA

Spatial interpolation and spatio-temporal interpolation can be used to analyze the overall deformation trend of the slope. In the process of interpolation, the selected variogram model is usually subject to subjective factors, theoretical semi-variograms, and parameters estimation. Then the universality and accuracy of interpolation methods will be affected to some extent.

In the computational process, the determination of spatio-temporal variation function sequence is actually a combinatorial optimization problem whose essence is NP-hard problem in optimization theory. However, due to discontinuity of the solution vector space and the difficulty in the solution neighborhood representation, it is difficult to calculate the results using classical algorithm. Then, as one of the modern optimization algorithms, the main feature of the genetic algorithm is that it can jump out of the local optimal solution with probability 1 for the nonlinear extremum problems and find the global optimal solution. It is a heuristic algorithm. The characteristic of skipping local optimum and searching for global optimum is mainly determined by crossover and mutation behaviors. References [43]–[45] have proposed an improved self-adaptive genetic algorithm for better search capacity, convergence and stability. On the basis, this paper proposes ISTKIA based on IAGA, and its calculation flow is shown in Fig.1:

The basic idea of ISTKIA based on IAGA could be explained as follows:

1) CODING MODE

Generally, chromosome coding methods include floating-point coding, binary coding, gray coding and symbol coding. Among them, the floating-point coding can represent wide range and high precision values. It is more convenient for genetic searching in larger space, and can better represent the time-series relationship of the Kriging interpolation

variogram and long-time series of slope surface. Therefore, it was selected in this paper for representation.

Firstly, according to actual situations of the mine slope, the obtained monitoring data of the slope were grouped by period and coded according to time series by the spatio-temporal Kriging variogram. Each group contained the spatial variogram function and the time variogram function in a certain period. In addition, the historical data were divided into t periods. The specific coding mode is shown in Fig.2:

$$\underbrace{l_{11}\ l_{12}}_{\text{1st period}}\quad \underbrace{l_{21}\ l_{22}}_{\text{2nd period}}\quad \underbrace{l_{31}\ l_{32}}_{\text{3rd period}}\quad \cdots\quad \underbrace{l_{m1}\ l_{m2}}_{m\text{-th period}}\quad \cdots\quad \underbrace{l_{t1}\ l_{t2}}_{t\text{-th period}}$$

FIGURE 2. Time series coding mode of the spatio-temporal Kriging variogram.

In Fig.2, $l_{m1}l_{m2}$, the *m-th* chromosome set, represents the spatial variogram function code l_{m1}(its range is 1-*i*, and the coded numbers refer to the adopted spatial variogram models, such as spherical models, exponential models, etc.) and the time variogram function code l_{m2}(its range is 1-*j*, and the coded numbers refer to the adopted time variogram models) in the m-th period. It should be noted that when i and j are more than single digits, $l_{m1}l_{m2}$ could increase the length of the chromosome to indicate its coding range according to actual situations.

2) INITIAL POPULATION

Generally speaking, the initial population should be large enough to improve the probability of the optimal solution. The larger the scale, the wider the searching range, and the longer the genetic process of offspring is. In addition, the quality of the initial total group also directly affects the accuracy of the results and the efficiency of the algorithm. Therefore, in the determination of the initial variogram, the empirical model can be used firstly. On the other hand, some classical optimization algorithms, such as the improved circle algorithm based on Hamilton, can be used to optimize the initial population and obtain a better parent.

3) GENETIC CROSS AND VARIATION OF CHROMOSOMES

The chromosome cross matching of IAGA based on Kriging compile function time series will be carried out in a suitable way. That is, the order of the population should be determined according to the fitness degree of the samples. Parents with low fitness match with each other, and parents with high fitness match with each other. Then the location of the intersection will be determined according to the logistic chaotic sequence. Finally, crossover operation will be conducted for the parents who need cross pairing according to their positions.

In practice, a crossover probability value P_j which is generally between 0-1 can be set first. In general, when $P_j = 1$, it means that crossover operations have been performed on all individuals. When $P_j = 0$, it means that no crossover operations have been implemented. A uniformly distributed random number obeying 0-1should be generated at each time. Then if the random number is greater than P_j, it is necessary to perform the corresponding operations on the corresponding individual genomic set point.

Similar to the crossover operation, the mutated individual can be selected from the individuals after the crossover operation. A crossover probability value N_b which is generally between 0-1 should be preset. The sample capacity is assumed to be N, and the number of variants is $N_b = N_b^* N$.

4) ADAPTIVE OPTIMIZATION OF CROSSOVER PROBABILITY AND MUTATION PROBABILITY

In order to improve the quality of the offspring optimal solution and reduce the probability of the local optimal solution, the genetic mutation probability can be adaptively corrected to avoid falling into local extremum during the search in the large spatial range of the variogram time series [54]. Therefore, Eq.7 and Eq.8 were used to correct it.

$$p_j = \begin{cases} p_{j_0} - \alpha(f_j - f_{aver})/(f_{aver} - f_{\max}), & f_j > f_{aver} \\ p_{j_0}, & f_j < f_{aver} \end{cases} \tag{7}$$

$$p_b = \begin{cases} p_{b_0} - \beta(f_b - f_{aver})/(f_{aver} - f_{\max}), & f_b > f_{aver} \\ p_{b_0}, & f_b < f_{aver} \end{cases} \tag{8}$$

In Eq.7 and Eq.8, p_{j_0} and p_{b_0} are fixed constants and often used to indicate the initial crossover probability and the mutation probability. α and β are constants with interval [0,1], f_j is the maximum fitness in the cross-parent, f_b is the maximum fitness of the mutant individual, f_{aver} is the average fitness of all individuals, and f_{max} is the maximum fitness among all individuals.

5) DETERMINATION OF THE OBJECTIVE FUNCTION

Assuming that the time-series chromosome of the spatio-temporal Kriging interpolation variogram of the open-pit mine slope surface was composed of T periods. When the variogram type was modified during a certain period, the performance of the Kriging interpolation would change accordingly, and then another set of variogram sequences would be found to optimize the interpolation effect. Then, the minimum R_{MSE} after interpolation in the slope surface area was taken as the target by cross-validation, and the objective function was determined as Eq.9:

$$\min = \frac{\sum_{i=1}^{T}\sum_{j=1}^{n_i} sqrt[(x_{ij} - x_{ij}^0)^2 + (y_{ij} - y_{ij}^0)^2 + (z_{ij} - z_{ij}^0)^2]}{\sum_{i=1}^{T}\sum_{j=1}^{n_i}} \tag{9}$$

where T is the time period of the variogram sequence, n_i is the number of the known points of the slope in the i-th period, and (x_{ij}, y_{ij}, z_{ij}) is the point coordinate obtained by Kriging interpolation. $(x_{ij}^0, y_{ij}^0, z_{ij}^0)$ is the original coordinate of the point obtained by Kriging interpolation. Denominator represents the number of all known monitoring points in

the time period. Therefore, the mathematical meaning of the objective function is the average value of the root mean square error, that is, the smaller the objective function, the greater the individual's fitness.

III. INTERPOLATION PRECISION ANALYSIS

A. STUDY AREA AND DATA SOURCE

In this paper, the Yuebao open-pit mine was taken as the research object. Located in Tanbu Town, Huadu District, Guangzhou City, China, it is about 2 km away from the West 2nd Ring Highway on the north side and about 780 m away from the provincial road S267. Its geographical coordinates are 113°4'19'' E and 23°17'50'' N, as shown in Fig.3. In October 2016, landslides occurred on the HP1 slope of the mining area under the influence of continuous rainfall and infiltration of the surface fishpond water. The length of the slope is about 175 m and the total inclination is about 60°. The elevation is from -73.66 m to -11.40 m and the height difference of rock slope is about 62.3 m. The gradient is about from 45° to 55°, while the gradient on the top s about 20° [47]. In order to analyze the stability of HP1 slope and ensure the safety production and management of the mine, 40 deformation monitoring points, numbered JC01-JC40 were set up according to the actual situations of the slope, constituting 5 deformation observation lines, as shown in Fig.4. Considering the actual situation of the slope and the safety of the monitoring point arrangement worker, some platforms had few monitoring points. In order to better analyze the slope deformation trend and improve the deformation accuracy, the monitoring points were densified around the observation line near the landslide area. Leica TM30 with high accuracy and stability was used to obtain

FIGURE 3. Location of Yuebao open-pit mine.

three-dimensional coordinates of each monitoring point, and the horizontal and settlement displacement were calculated.

B. ANALYSIS OF RESULTS

In order to compare and analyze the accuracy of the interpolation more clearly, the cross-validation method was used to evaluate its accuracy and test the quality of the determined variogram model. The basic ideas are as follows.

First, the observed values $Z(x_i)(i = 1, 2, \ldots, n)$ were removed from the monitoring data column, then the variogram model was established by using the remaining observation values, and the estimated value $Z^*(x_i)$ of the removed monitoring point was predicted. Meanwhile, $Z^*(x_i)$ values were returned to the original data column, and the other points were selected to repeat the above operations until the estimated values of all the monitoring points were calculated. Finally, the error d_{Zi} between the original data and the estimated value was calculated to analyze the consistency of the data. The R_{MSE} was obtained according to Eq.10 to test the accuracy of the interpolation. Meanwhile, the correlation degree was evaluated by the coefficient R^2. The calculation expression is shown in Eq.11. When R^2 was approximately 1, the correlation between the two values was stronger. The flow of calculation steps is shown in Fig.5.

$$R_{\mathrm{MSE}} = \sqrt{\frac{\sum_{i=1}^{n} (Z - Z^*)^2}{n}} \tag{10}$$

$$R^2 = 1 - \frac{S_{res}}{S_{total}} \tag{11}$$

In Eq.11, S_{res} and S_{total} are the sum of the squared residuals and the total sum of squares, respectively. The calculation functions are shown in Eq.12 and Eq.13.

$$S_{\mathrm{res}} = \sum_{i=1}^{n} (Z - Z^*)^2 \tag{12}$$

$$S_{\mathrm{total}} = \sum_{i=1}^{n} (Z - \overline{Z})^2 \tag{13}$$

In Eq.13, $\bar{Z}$ is the average of the sample points.

In order to verify the feasibility of ISTKIA based on IAGA, the collected deformation monitoring data were divided into three periods (December 23, 2016, May 31, 2017 and February 07, 2018). The missing data were interpolated by the spatial Kriging method, the spatio-temporal Kriging method, the spatio-temporal method of Gaussian process regression and the ISTKIA based on IAGA. Four interpolation errors were obtained as shown in Table 1 according to cross-validation. In addition, the residual distribution of the ISTKIA is shown in Fig. 6.

Therefore, according to the cross-validation results of Table 1 and the residual distribution of Fig.5, the conclusions can be drawn:

1) The ISTKIA based on IAGA overcomes limitations of the variogram model subjected to subjective factors,

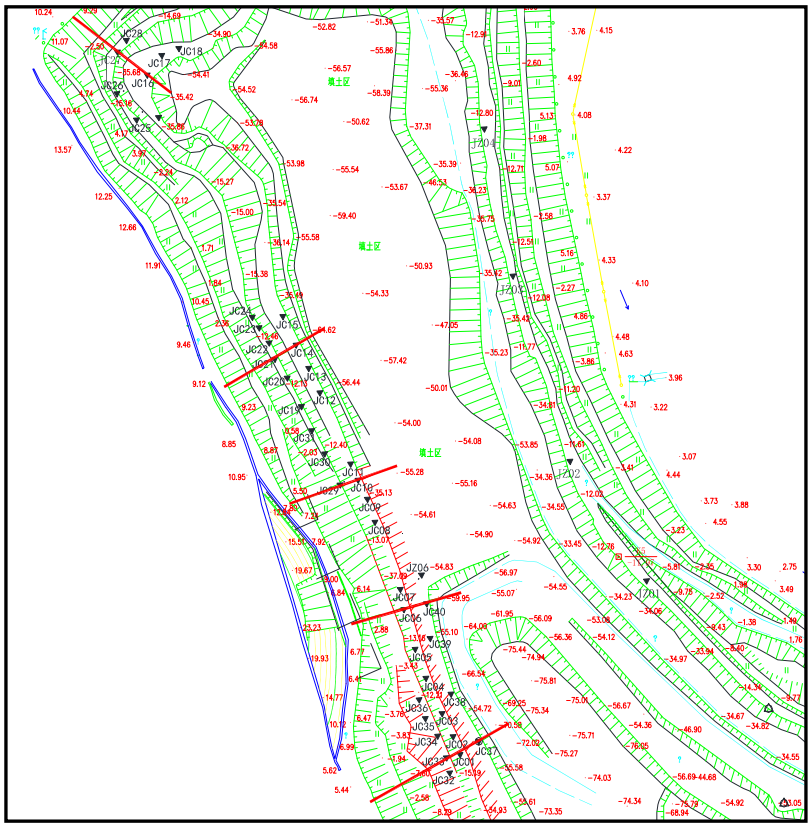

FIGURE 4. Distribution of monitoring points on the slope in Yuebao open-pit mine.

TABLE 1. Comparison of root mean square error and correlation coefficient of the spatio-temporal Kriging in different monitoring periods.

NO.	Time	The spatial Kriging interpolation		The traditional spatio-temporal Kriging interpolation		The spatio-temporal interpolation of Gaussian process regression		The ISTKIA based on IAGA	
		R_{MSE} (m)	R^2	R_{MSE} (m)	R^2	R_{MSE} (m)	R^2	R_{MSE} (m)	R^2
1	Dec. 23, 2016	0.121	0.932	0.09	0.961	0.086	0.971	0.050	0.999
2	May 31, 2017	0.136	0.847	0.100	0.885	0.092	0.901	0.048	0.999
3	Feb. 07, 2018	0.143	0.831	0.104	0.875	0.095	0.896	0.049	0.999

the theoretical semi-variogram and many estimated parameters. The interpolation accuracy is better than traditional spatio-temporal Kriging method and the spatio-temporal interpolation method of Gaussian process regression, increasing about 1 time. It shows that it has certain universality and reliability.

2) With the increasing amount of the slope monitoring data and the relatively large deformation change, the ISTKIA based on IAGA fully embodies the advantages of calculation adaptability in the optimization of the variogram model and the estimated parameters. It has better operation efficiency and higher interpolation precision.
3) The calculation accuracy of spatio-temporal interpolation method is significantly higher than that of the spatial interpolation method, regardless of the period of time, showing that the monitoring points not only have the spatial correlation, but also have strong spatio-temporal correlation. The interpolation results, consistent with the actual situations, fit the state of the slope monitoring points well. It is beneficial to the analysis of the whole deformation trend of the slope.

TABLE 2. Partial coordinates of JC09 and JC12.

Time	Coordinates of the monitoring points					
	JC09			JC12		
	x	*y*	*z*	*x*	*y*	*z*
23-Dec-16	1421.1378	349.2082	65.7563	1507.3468	339.8713	65.5426
20-Jan-17	1421.1427	349.2089	65.7544	1507.3484	339.8759	65.5414
25-Feb-17	1421.1446	349.2108	65.7543	1507.3495	339.8777	65.5400
28-Mar-17	1421.1508	349.2131	65.7540	1507.3526	339.8831	65.5396
15-Apr-17	**1421.1522**	**349.2120**	**65.7536**	**1507.3544**	**339.8852**	**65.5389**
1-May-17	1421.1553	349.2133	65.7527	1507.3535	339.8875	65.5393
15-May-17	1421.1535	349.2140	65.7525	1507.3551	339.8866	65.5388
18-Jun-17	1421.1583	349.2136	65.7522	1507.3591	339.8914	65.5373
21-Jul-17	1421.1587	349.2154	65.7515	1507.3601	339.8939	65.5374
25-Aug-17	**1421.1620**	**349.2174**	**65.7503**	**1507.3606**	**339.8984**	**65.5376**
8-Sep-17	1421.1617	349.2184	65.7517	1507.3616	339.8999	65.5380
3-Oct-17	1421.1651	349.2167	65.7522	1507.3609	339.8979	65.5368
5-Nov-17	1421.1631	349.2164	65.7516	1507.3606	339.8990	65.5374
8-Dec-17	1421.1607	349.2175	65.7504	1507.3615	339.8991	65.5381
10-Jan-18	1421.1650	349.2183	65.7524	1507.3627	339.9001	65.5369
7-Feb-18	1421.1640	349.2172	65.7527	1507.3602	339.8997	65.5371
10-Mar-18	1421.1629	349.2166	65.7518	1507.3596	339.8995	65.5378

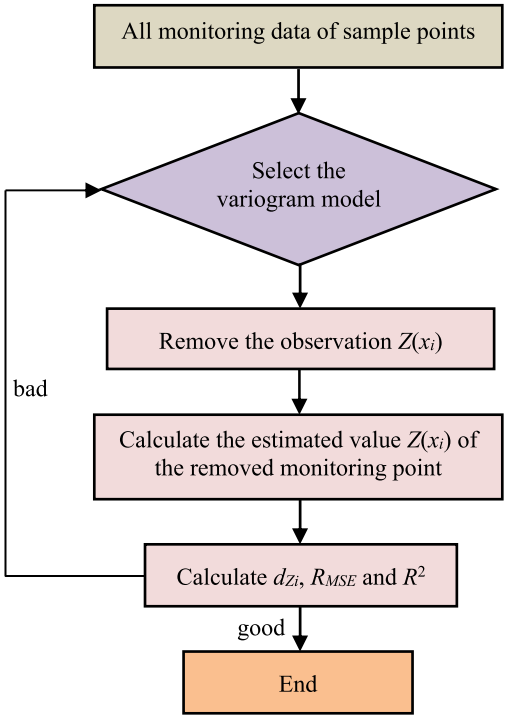

FIGURE 5. Calculation procedure of cross-validation.

4) According to the results of four interpolation methods, R^2 is consistent in three stages by ISTKIA based on IAGA, while it is different by the other three methods. It shows that the proposed ISTKIA has high stability and the interpolation results are feasible, and improves the accurate analysis of the change trend of monitoring points and the slope stability.

IV. SLOPE STABILITY AND DEFORMATION TRENDS ANALYSIS OF ISTKIA BASED ON IAGA

The accurate and complete deformation monitoring data are key to the analysis of slope stability and deformation trends, which is also the premise of safety production and management in mines. To solve the problem of data missing in actual monitoring, taking the HP1 slope as the research object, this paper interpolated the missing data of each monitoring point by using ISTKIA based on IAGA to ensure the continuity and integrity. However, considering many deformation monitoring points and large amount of monitoring data in the monitoring of HP1 slope as well as the paper length, only the missing coordinate values of JC09 and JC12 were calculated, and some of them were listed in Table 2. The data in the bold is the interpolation data. On this basis, the stability and the deformation trend of the HP1 slope were analyzed. The results could provide an important technical basis and decision support for the disaster prevention, reduction and relief of mine slopes.

Generally speaking, the commonly-used method to judge slope stability is to see whether the displacement of the monitoring point is more than its set warning threshold or control

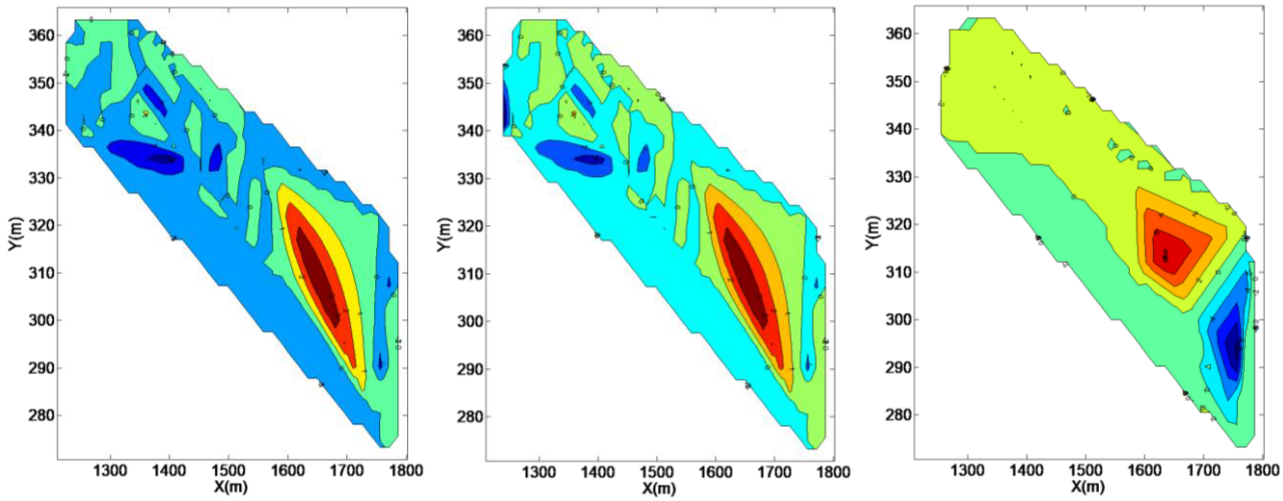

FIGURE 6. Distribution of interpolation residual in different monitoring periods.

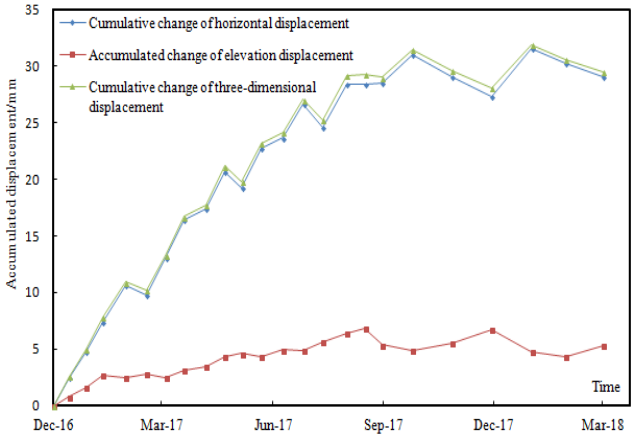

FIGURE 7. Accumulated displacement-time curve of JC09 for all directions.

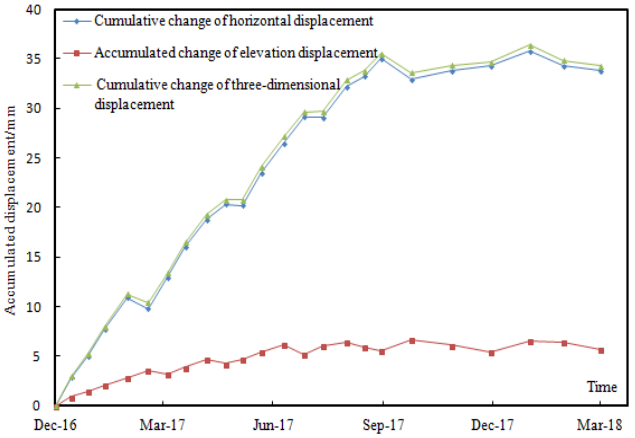

FIGURE 8. Accumulated displacement-time curve of JC12 for all directions.

threshold in the deformation monitoring analysis. When the accumulative displacement of the monitoring point is greater than its early warning threshold or control threshold, there is a high probability of slope instability. Therefore, setting a reasonable and effective early warning threshold or control threshold is the key to slope stability judgement. According to the above analyses, historical data and actual situations of the HP1 slope of the Yuebao open-pit mine, as well as relevant specifications and references [48], [49], the alarm threshold was set as 30mm, and the control threshold was set as 35mm. The rate of daily average displacement shall not exceed 2mm/d for three consecutive days. When the displacement monitoring data are less than the above parameters, the probability of slope instability is small. With a large number of deformation monitoring points, JC09 and JC12 monitoring points were taken as research objects to study the stability of the slope (as shown in Fig.7 and Fig.8).

According to the cumulative displacement-time curves of JC09 and JC12 in all directions, it can be seen that the displacement of each monitoring point shows an increasing trend in the early period (Dec. 2016 to Aug. 2017). The maximum deformation could be observed at JC12 monitoring point, and the maximum cumulative displacement is about 35.8mm, reaching the control threshold; JC09 comes second, with the maximum cumulative displacement of 31.5mm which exceeds the alarm threshold. The deformation of other monitoring points is less than the alarm threshold of 30mm, and the displacement deformation does not exceed 2mm/d for three consecutive days.

Suffering from continuous rainfall, the deformation of the monitoring points in some areas gradually increases from Dec. 2016 to Aug. 2017. There is a possibility of further slope instability, which needs primary focus, heightened vigilance and strengthened prevention and control. Under such conditions, on the premise of studying the influence of the rainfall on the slope stability [50]–[52], the corresponding prevention and control measures were taken to change physical and mechanical parameters such as friction angle, cohesion and groundwater level caused by the surface rainwater infiltration. With further slope treatments, the displacement

of each monitoring point on the HP1 slope basically slightly fluctuated up and down around the maximum cumulative displacement since Sep. 2017.

To sum up, although the cumulative displacement of the monitoring points on the HP1 slope was large in the early period, most of them failed to reach the alarm threshold. The cumulative displacement of all monitoring points didn't further expand after taking the corresponding treatment measures in the mine. The slope remained stable.

V. CONCLUSIONS

The analysis of slope stability through deformation monitoring data is an essential way to forecast and warn slope disasters. However, the scarce monitoring data in practical deformation monitoring couldn't meet the needs of scientific research and engineering applications and may bring deviations in slope stability analysis, which may further lead to mistakes in slope construction schemes and slope disaster prevention and control. To overcome the problems during the calculation by traditional method, such as varogram model and parameter estimation and etc., an improved spatio-temporal Kriging interpolation algorithm (ISTKIA) was developed in this paper with full consideration of spatio-temporal correlations among monitoring points. And it was successfully used to interpolate the missing monitoring data and analyze the HP1 slope stability. The main conclusions and contributions are as follows:

1) According to the calculation results, the ISTKIA based on IAGA is more universal and reliable in the time of optimal variogram and the calculated R_{MSE} and R^2 were significantly higher than those of the traditional spatio-temporal Kriging, increasing by about 1 time. It better overcomes limitations of traditional spatio-temporal Kriging methods, and improves the interpolation precision and calculation efficiency.
2) According to the deformation monitoring data and the interpolation results, the maximum cumulative displacement of the HP1 slope was about 35.8 mm at JC12, and the displacement deformation of all monitoring points didn't exceed 2mm/d for three consecutive days. Although the displacement reached the control threshold, all monitoring points were basically stable and weren't further enlarged through proper treatments. The deformation trend of each monitoring point was basically consistent with the actual slope. It shows that the ISTKIA based on IAGA is feasible and practical, and can be adopted to guide safety production and mines management.
3) To some extent, the ISTKIA makes up for and overcomes the missing, discontinuity and unevenness of the slope monitoring data, as well as ensures the integrity of the monitoring data and the effective analysis of the monitoring points change trend. It provides an important technical basis and decision support for the disaster prevention, reduction and relief of mine slopes, and a new idea for the research of the related problems in related fields.
4) In practical deformation monitoring, due to economic and external factors, the monitoring points are usually composed of dozens of points, which can not accurately describe the slope surface. The ISTKIA based on IAGA solves the problem of scarce and missing monitoring data of the slope surface. It can effectively analyze the whole spatio-temporal evolution law of the slope, improve work efficiency of employees and reduce the production cost of enterprises.
5) With the increasing amount of the monitoring data, the initial calculation data should be increased in the later data processing, in order to optimize the calculation model, ensure interpolation precision and improve accuracy and reliability of the slope stability analysis.

REFERENCES

[1] H. Xiao, "Dynamic evaluation method and application of slope stability in small and medium open-pit mines," Ph.D. dissertation, School Environ. Sci. Spat. Inform., CUMT, Xuzhou, China, 2019.
[2] Z. Zou, G. Liu, and S. Wen, "Slope stability evaluation method based on improved fuzzy clustering iteration," *J. Jiangxi Univ. Sci. Technol.*, vol. 39, no. 1, pp. 11–15, Feb. 2018.
[3] D.-S. Xu, L.-J. Dong, L. Borana, and H.-B. Liu, "Early-warning system with quasi-distributed fiber optic sensor networks and cloud computing for soil slopes," *IEEE Access*, vol. 5, pp. 25437–25444, Dec. 2017.
[4] Y. Mao, H. Chen, and Z. Li, "Application of uncertain fuzzy ID3 decision tree in the evaluation of landslide hazard," *J. Jiangxi Univ. Sci. Technol.*, vol. 38, no. 5, pp. 92–98, Oct. 2017.
[5] B. Hu, G. Su, J. Jiang, J. Sheng, and J. Li, "Uncertain prediction for slope displacement time-series using Gaussian process machine learning," *IEEE Access*, vol. 7, pp. 27535–27546, 2019.
[6] K. Zhao, L. Yu, and H. Shao, "Research on rock slope stability in the condition of rainfall or blasting vibration," *J. Jiangxi Univ. Sci. Technol.*, vol. 36, no. 1, pp. 43–48, Feb. 2015.
[7] S. Wang, T. Zhou, Y. Ji, and X. Sun, "A method of slope deformation monitoring based on GPS carrier phase," *Sci. Tech. Eng.*, vol. 17, no. 25, pp. 84–88, Sep. 2017.
[8] H. Wu, C. Huang, and J. Ye, "Deformation monitoring system for high slope in open-pit mine with the integration of GNSS and GIS," *Geomat. Inf. Sci. Wuhan Univ.*, vol. 40, no. 5, pp. 706–710, May 2015.
[9] F. Gerber, R. de Jong, M. E. Schaepman, G. Schaepman-Strub, and R. Furrer, "Predicting missing values in spatio-temporal remote sensing data," *IEEE Trans. Geosci. Remote Sens.*, vol. 56, no. 5, pp. 2841–2853, May 2018.
[10] A. Sekulić, M. Kilibarda, D. Protić, M. P. Tadić, and B. Bajat, "Spatio-temporal regression kriging model of mean daily temperature for Croatia," *Theor. Appl. Climatol.*, vol. 140, pp. 101–114, Dec. 2019.
[11] D.-G. Hu and H. Shu, "Spatiotemporal interpolation of precipitation across Xinjiang, China using space-time CoKriging," *J. Central South Univ.*, vol. 26, no. 3, pp. 684–694, Mar. 2019.
[12] J. Cui, "The space–time distribution of soil water and temperature of a desert ecosystem using spatio-temporal kriging and PCA analysis," *J. Indian Soc. Remote Sens.*, vol. 48, no. 2, pp. 271–286, Feb. 2020.
[13] X. Yang, Y. Yang, and E. Li, "Spatial-temporal interpolation of PM 2.5 based on space-temporal regression kriging and AOD data," *Adm. Techn. Envir. Monit.*, vol. 31, no. 6, pp. 12–16, Dec. 2019.
[14] M. Wang and J. Chen, "Simulation of pollutant dispersion in exponential spatial-temporal interpolation based on genetic algorithm," *Water Resour. Power*, vol. 35, no. 1, pp. 35–38, Jan. 2017.
[15] O. E. Abe, A. B. Rabiu, O. S. Bolaji, and E. O. Oyeyemi, "Modeling African equatorial ionosphere using ordinary kriging interpolation technique for GNSS applications," *Astrophys. Space Sci.*, vol. 363, no. 8, p.168 , Aug. 2018.
[16] Y. Mao, H. Cao, and J. He, "Spatio-temporal integrated forecasting algorithm for dam deformation," *Comput. Sci.*, vol. 46, no. 2, pp. 232–238, Feb. 2019.

[17] H. Shen, X. Li, Q. Cheng, C. Zeng, G. Yang, H. Li, and L. Zhang, "Missing information reconstruction of remote sensing data: A technical review," *IEEE Geosci. Remote Sens. Mag.*, vol. 3, no. 3, pp. 61–85, Sep. 2015.
[18] H. Yang, T. Li, and Z. Zhang, "Application of metabolic model in slope displacement monitoring by Lagrange interpolation method," *Saf. Environ. Eng.*, vol. 24, no. 2, pp. 33–38, Mar. 2017.
[19] H. Wen and P. Yang, "Application of GM(1, 1)model based on Hermite interpolation method in prediction of soft foundation surface subsidence," *Port Wat. Eng.*, no. 3, pp. 47–51, Mar. 2015.
[20] Y. Liu, Y. Duan, and L. Guan, "Cubic spline interpolation method and its application in deformation data preprocessing," *Site Invest Sci. Technol.*, vol. 6, pp. 47–50, 2017.
[21] S. Khan, D.-H. Lee, M. A. Khan, A. R. Gilal, and G. Mujtaba, "Efficient edge-based image interpolation method using neighboring slope information," *IEEE Access*, vol. 7, pp. 133539–133548, 2019.
[22] J. Wang, Q. Sun, and S. Du, "The application of kriging spatial interpolation method in monitoring surface deformation," *China Land Sci.*, vol. 27, no. 12, pp. 87–91, Dec. 2013.
[23] P. Bogaert, "Comparison of kriging techniques in a space-time context," *Math. Geol.*, vol. 28, no. 1, pp. 73–86, Jan. 1996.
[24] Y. Liu, Z. Chen, B. Hu, J. Jin, and Z. Wu, "A non-uniform spatiotemporal kriging interpolation algorithm for landslide displacement data," *Bull. Eng. Geol. Environ.*, vol. 78, no. 6, pp. 4153–4166, Sep. 2019.
[25] G. Lenda, M. Ligas, P. Lewińska, and A. Szafarczyk, "The use of surface interpolation methods for landslides monitoring," *KSCE J. Civil Eng.*, vol. 20, no. 1, pp. 188–196, Jan. 2016.
[26] W. Jianmin and Z. Jin, "Deformation intelligent prediction model based on Gaussian process regression and application," *Geomatics Inf. Sci. Wuhan Univ.*, vol. 43, no. 2, pp. 248–254, Feb. 2018.
[27] J. Wang, J. Zhang, Z. Deng, and Y. Wang, "Slope deformation analyses with space-time kriging interpolation method," *J. China Coal Soc.*, vol. 39, no. 5, pp. 874–879, May 2014.
[28] Z. Zhang, Y. Wang, and H. Yan, "A spatio-temporal hybrid interpolation method and its application," *Sci. Surv. Mapp.*, vol. 41, no. 12, pp. 265–270, Dec. 2016.
[29] H. Sun, L. Hou, G. Zong, and X. Yu, "Fixed-time attitude tracking control for spacecraft with input quantization," *IEEE Trans. Aerosp. Electron. Syst.*, vol. 55, no. 1, pp. 124–134, Feb. 2019.
[30] G. Zong, W. Qi, and H. R. Karimi, "L_1control of positive semi-Markov jump systems with state delay," *IEEE Trans. Syst., Man, Cybern. Syst.*, early access, Mar. 24, 2020, doi: 10.1109/TSMC.2020.2980034.
[31] G. Zong and H. Ren, "Guaranteed cost finite-time control for semi-Markov jump systems with event-triggered scheme and quantization input," *Int. J. Robust Nonlin.*, vol. 29, no. 15, pp. 5251–5273, 2019.
[32] H. Ren, G. Zong, and H. R. Karimi, "Asynchronous finite-time filtering of networked switched systems and its application: An event-driven method," *IEEE Trans. Circuits Syst. I, Reg. Papers*, vol. 66, no. 1, pp. 391–402, Jan. 2019.
[33] Y. Seo, S. Kim, and V. P. Singh, "Estimating spatial precipitation using regression kriging and artificial neural network residual kriging (RKNNRK) hybrid approach," *Water Resour. Manage.*, vol. 29, no. 7, pp. 2189–2204, May 2015.
[34] X. Li, H. Shen, R. Feng, J. Li, and L. Zhang, "DEM generation from contours and a low-resolution DEM," *ISPRS J. Photogramm. Remote Sens.*, vol. 134, pp. 135–147, Dec. 2017.
[35] Y. Zhao, Z. Sun, and J. Chen, "Analysis and comparison in arithmetic for kriging interpolation and sequential Gaussian conditional simulation," *Geo-Inf. Sci.*, vol. 12, no. 6, pp. 767–776, Jan. 2011.
[36] Z. Han, "Kriging surrogate mode and its application to design optimization: A review of recent progress," *Acta Aeronaut. Astronaut. Sin.*, vol. 37, no. 11, pp:3197-3225, Mar. 2016.
[37] L. Zhao, K. K. Choi, and I. Lee, "Metamodeling method using dynamic kriging for design optimization," *AIAA J.*, vol. 49, no. 9, pp. 2034–2046, Sep. 2011.
[38] H. Liang, M. Zhu, and Z. Wu, "Using cross-validation to design trend function in kriging surrogate modeling," *AIAA J.*, vol. 52, no. 10, pp. 2313–2327, Oct. 2014.
[39] Q. He, J. Wang, and J. Ao, "Optimization of disaster base station network based on IAGA model," *Bull. Surv. Map.*, vol. 8, pp. 7–12, Aug. 2017.
[40] M. Xu, T. Xing, and M. Han, "Spatial-temporal data interpolation based on spatial-temporal kriging method," *Acta Automatica Sin.*, vol. 44, pp. 1–8, 2018. [Online]. Available: http://kns.cnki.net/kcms/detail/11.2109.TP.20180503.1719.006.html
[41] S. O. Ahmed, R. Mazloum, and H. Abou-Ali, "Spatiotemporal interpolation of air pollutants in the greater Cairo and the Delta, Egypt," *Environ. Res.*, vol. 160, pp. 27–34, Jan. 2018.
[42] L. Fontanella, L. Ippoliti, R. J. Martin, and S. Trivisonno, "Interpolation of spatial and spatio-temporal Gaussian fields using Gaussian Markov random fields," *Adv. Data Anal. Classification*, vol. 2, no. 1, pp. 63–79, Apr. 2008.
[43] B. Li, X. Xiao, and L. Zhang, "Study on sectional optimization of gabled frames based on improved genetic algorithm," *J. Jiangxi Univ. Sci. Technol.*, vol. 39, no. 5, pp. 9–14, Oct. 2018.
[44] S. Liu, T. Jin, and L. Wang, "An improved adaptive genetic algorithm," *J. Jiangxi Univ. Sci. Technol.*, vol. 31, no. 1, pp. 59–62, Feb. 2010.
[45] T. Jiao, G. Zong, S. K. Nguang, and C. Zhang, "Stability analysis of genetic regulatory networks with general random disturbances," *IEEE Trans. Nanobiosci.*, vol. 18, no. 2, pp. 128–135, Apr. 2019.
[46] G. Yu and X. Yu, "An improved adaptive genetic algorithm," *J. Math. Pract. Theory*, vol. 45, no. 19, pp. 259–264, Nov. 2015.
[47] H. Xiao, G. Guo, and L. Chen, "Research on dynamic evaluation model of slope risk based on improved VW-UM," *Math. Problems Eng.*, vol. 2019, pp. 1–13, Feb. 2019.
[48] B. Yang, "Slope deformation monitoring scheme," B.S. thesis, Coll. Munic. Mapp. Eng., Hunan City Univ., Yiyang, China, 2012.
[49] Z. Yang, "Slope displacement monitoring and control," *China Min. Eng.*, vol. 35, no. 4, pp. 43–46, Aug. 2006.
[50] M. Suradi, A. B. Fourie, and M. J. Saynor, "An experimental and numerical study of a landslide triggered by an extreme rainfall event in northern australia," *Landslides*, vol. 13, no. 5, pp. 1125–1138, Oct. 2016.
[51] C.-M. Lo, C.-F. Lee, and W.-K. Huang, "Failure mechanism analysis of rainfall-induced landslide at Pingguang stream in taiwan: Mapping, investigation, and numerical simulation," *Environ. Earth Sci.*, vol. 75, no. 21, p. 1422, Nov. 2016.
[52] Y. Mao, Z. Zhou, Z. Peng, and X. Gao, "Landslide hazard prediction based on uncertain multi-classification support vector machine method," *J. Jiangxi Univ. Sci. Technol.*, vol. 37, no. 3, pp. 102–108, Jun. 2016.

HAIPING XIAO received the B.Eng. degree in surveying and mapping engineering from the Jiangxi University of Science and Technology, Ganzhou, China, in 2004, and the Ph.D. degree in geodesy and surveying engineering from the China University of Mining and Technology, Xuzhou, China, in 2019. His current research interests include deformation monitoring and data processing and slope stability analysis and evaluation.

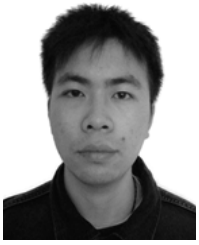

ZHENCHAO ZHANG received the B.Eng. degree in civil engineering from the College of Applied Sciences, Jiangxi University of Science and Technology, Ganzhou, China, in 2019. He is currently pursuing the M.A.S. degree with the School of Architecture and Surveying and Mapping Engineering, Jiangxi University of Technology. His current research interests include deformation monitoring and data processing and slope stability analysis and evaluation.

LANLAN CHEN received the B.Eng. degree in civil engineering from Chongqing Jiaotong University, Chongqing, China, in 2005, and the M.A.S. degree in geodesy and surveying engineering from the Jiangxi University of Science and Technology, Ganzhou, China, in 2008. Her current research interests include deformation monitoring and data processing, and slope stability analysis and evaluation.

QIMIN HE received the B.Eng. degree in surveying and mapping engineering from the Jiangxi University of Science and Technology, Ganzhou, China, in 2015. He is currently pursuing the Ph.D. degree with the School of Environment Science and Spatial Informatics, China University of Mining and Technology, Xuzhou, China. His current research interests include GNSS meteorology and atmosphere monitoring.